

## Observation of Modulational Instability in Optical Fibers

K. Tai, A. Hasegawa, and A. Tomita

*AT&T Bell Laboratories, Murray Hill, New Jersey 07974*

(Received 19 August 1985)

We report the first observation of the modulational instability of light waves in dielectric material using a neodymium-doped yttrium aluminum garnet laser operated at 1.319  $\mu\text{m}$  and single-mode optical fibers with anomalous group-velocity dispersion. The observed results are in good agreement with the theoretical predictions. The relationship between the modulation instability and parametric four-wave mixing and the interplay with stimulated Raman and Brillouin scatterings are also presented.

PACS numbers: 42.65.-k

Modulational instability is a process in which the amplitude and phase modulations of a wave grow as a result of an interplay between the nonlinearity and anomalous dispersion. The process is analogous to the trapping of a quasiparticle in a potential generated by its own intensity [see Eq. (1) in the following]. Modulational instability has been studied for waves in fluids,<sup>1</sup> plasmas,<sup>2</sup> and dielectric media.<sup>3</sup> Hasegawa and Brinkman<sup>4</sup> have analyzed the modulational instability of light waves in a glass fiber. However, to our knowledge, there has been no experimental verification of modulational instability for an electromagnetic wave in a dielectric material. In this paper, we report the first experimental observation of the modulational instability using single-mode fibers. We study the dependence of the modulation frequency upon the fiber parameters and the laser power. Threshold powers are compared for the onset of the modulational instability and the stimulated Raman scattering.

The wave propagation in the lossless fiber in the group-velocity coordinate is described by the nonlinear Schrödinger equation<sup>5</sup>:

$$i \frac{\partial \mathcal{E}}{\partial z} = -\frac{k''}{2} \frac{\partial^2 \mathcal{E}}{\partial \tau^2} + \frac{\omega n_2}{2c} |\mathcal{E}|^2 \mathcal{E}, \quad (1)$$

where  $\mathcal{E}$  is the complex electric-field amplitude for the light-wave envelope,  $\omega$  is the angular frequency,  $z$  is the distance of transmission,  $\tau = t - z/v_g$ ,  $t$  is the time,  $v_g = (\partial k / \partial \omega)^{-1}$  is the group velocity,  $n_2 (= 1.22 \times 10^{-22} \text{ m}^2/\text{V}^2$  for silica<sup>6</sup>) is the Kerr coefficient, and  $k'' = \partial^2 k / \partial \omega^2$ .<sup>7</sup> It has been shown<sup>4</sup> that the cw solution  $\mathcal{E}_0(z)$  of Eq. (1),

$$\mathcal{E}_0(z) = \mathcal{E}_0 \exp[-i(\omega n_2 / 2c) |\mathcal{E}_0|^2 z], \quad (2)$$

is unstable for a small perturbation (or modulation)  $\mathcal{E}_1$ , where  $|\mathcal{E}_1| \ll |\mathcal{E}_0|$  and  $\mathcal{E}_1 \propto \exp[i(Kz - \Omega t)]$ . Plugging the perturbed electric field

$$\mathcal{E}(z, \tau) = \mathcal{E}_0 + \mathcal{E}_1(z, \tau) \exp[-i(\omega n_2 / 2c) |\mathcal{E}_0|^2 z]$$

into Eq. (1) with some mathematical manipulations, one can obtain the dispersion relation for the modulation wave number  $K$  and modulation frequency  $\Omega$  as

follows:

$$K^2 = \left( \frac{K'' \Omega^2}{2} \right)^2 \left[ 1 + \frac{2\omega n_2 |\mathcal{E}_0|^2}{ck'' \Omega^2} \right]. \quad (3)$$

It is apparent that if  $k'' n_2$  is negative and for the modulation frequency

$$\Omega < \Omega_c \equiv [(2\omega/c) |(n_2/k'') \mathcal{E}_0^2|]^{1/2},$$

$K$  becomes purely imaginary and the perturbation grows exponentially. The maximum amplitude growth rate is equal to  $(\omega/2c) n_2 |\mathcal{E}_0|^2$ , which is independent of fiber dispersion and is solely proportional to the light intensity, and occurs at  $\Omega = \Omega_c / \sqrt{2}$ , which is proportional to the square root of power divided by dispersion. It was further shown<sup>4</sup> that the instability develops frequency modulations whose  $n$ th sideband amplitude is proportional to  $E_0^n$  and is separated from the carrier frequency by  $n \Omega_c / \sqrt{2}$ ,  $n = 1, 2, \dots$

In the experiments, we use light from a mode-locked Nd-doped yttrium aluminum garnet laser operated at 1.319  $\mu\text{m}$ . The laser puts out 100-psec (FWHM) transform-limited pulses at a 100-MHz repetition rate. The fluctuation in the power is less than 5%. Since the expected modulation period is on the order of 2 psec, these pulses provide a quasi-cw condition. We take the approach of introducing no initial perturbation.<sup>8</sup> Instead, we detect the stimulated modulational instability (i.e., amplified spontaneous emission), which builds up from the spontaneous noise as a result of the exponential gain and is expected to occur at the modulation frequency of the maximum gain. A spectrometer and a second-harmonic autocorrelator are used for monitoring the modulation frequency and the corresponding period.

We use two sets of fibers. The first<sup>9</sup> has  $-2.4$ -psec/nm-km dispersion (zero dispersion at 1.29  $\mu\text{m}$ ), and consists of 0.5-, 1-, and 2-km lengths. The second<sup>10</sup> has  $-3.75$ -psec/nm-km dispersion (1.275  $\mu\text{m}$ ), and consists of 0.5- and 1-km lengths. We have observed the modulational instability in all of them.

Figure 1 shows typical power spectra as a function of power in the fiber. The fiber parameters are as fol-

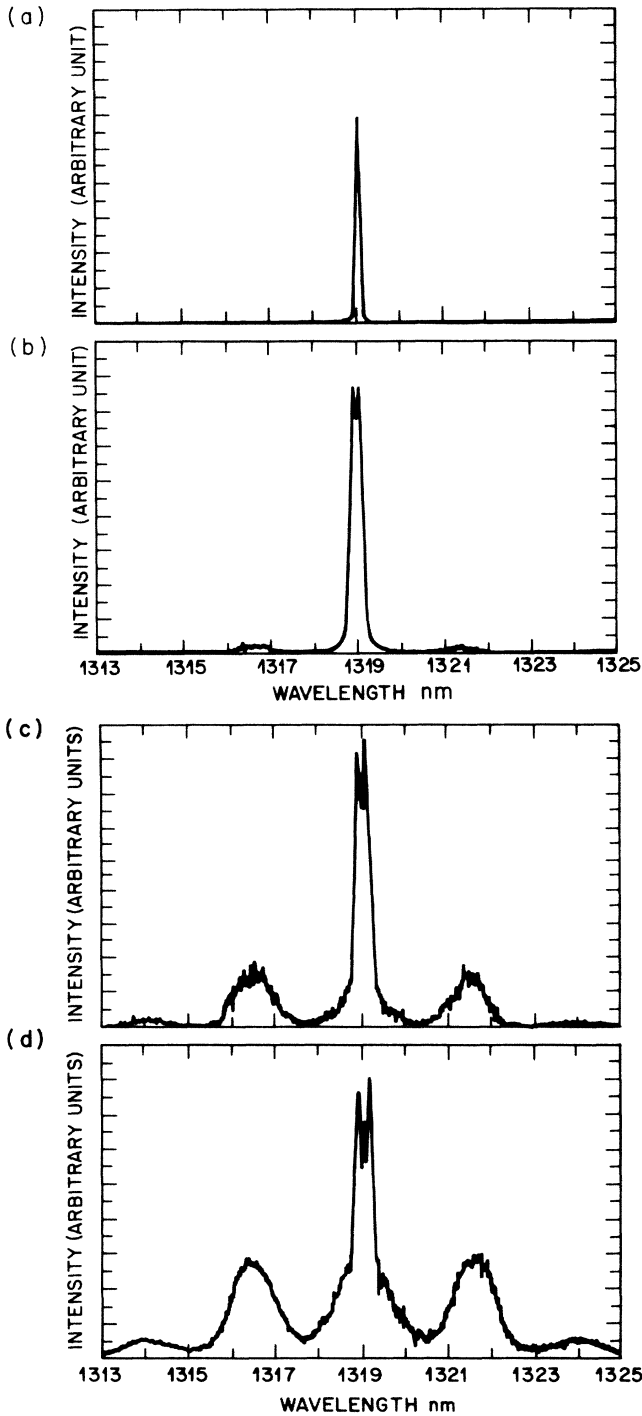


FIG. 1. A series of power spectra measured at the output end of the fiber as a function of the peak power: (a) low-power (or input) case, (b) 5.5 W, (c) 6.1 W, and (d) 7.1 W. The vertical scales in (b), (c), and (d) have the same normalization factor. The modulation-frequency sidebands are clearly shown in (b), (c), and (d).

lows:  $-2.4$ -psec/nm-km dispersion, 1-km length,  $60\text{-}\mu\text{m}^2$  geometric core size,  $0.67$ -dB/km loss at  $1.319\text{ }\mu\text{m}$ . The fiber power is varied by adjustment of the

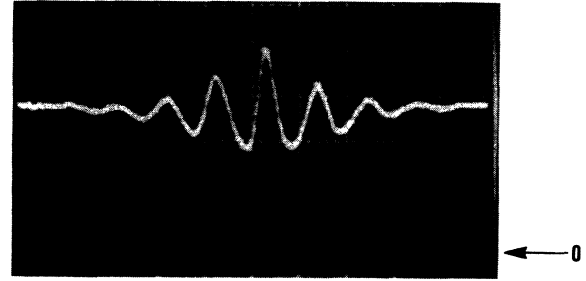


FIG. 2. A typical autocorrelation trace in the presence of the modulational instability. The zero delay occurs at the central maximum. The zero for the vertical axis is marked by an arrow. The interval between the oscillation peaks, which corresponds to the modulation period, is  $2.2$  psec in this case.

axial position of the  $20\times$  coupling-microscope objective. The peak value is obtained by multiplying the time-averaged power, measured at the output end of the fiber, by a duty cycle of 100. Figure 1(a) shows the spectrum for the low-power case, which is indistinguishable from the laser spectrum. Figure 1(b) shows the emergence of two symmetrical sidebands at  $5.5$  W peak power. Theory predicts a power gain of  $\exp(16)$  for this case, which accounts for the observation.<sup>11</sup> Figure 1(c) shows the growth of two sidebands and the emergence of the predicted secondary sidebands at  $6.1$  W. The height of the primary sidebands is about 6 times taller, while the increase in power is only 11%. This is a clear evidence of exponential gain. Figure 1(d) shows the further growth of these sidebands at  $7.1$  W. Considerable amount of pump depletion is shown. The broadening and the splitting of the central peak in Fig. 1 are due to the self-phase modulation of the  $100$ -psec finite duration in the input pulses.<sup>6</sup> The finite width in the sidebands is partly because the instability starts from spontaneous emission, and partly because the laser pulse is not rectangularlike. Figure 2 shows a typical autocorrelation trace. The observed period corresponds to the inverse of the sideband frequency very well. The limited modulation depth and the damping in the oscillation of the autocorrelation trace are due to the finite width of the spectral peaks.

Figure 3 shows the modulation period as a function of fiber power and dispersion. The triangles and circles are experimental data; the solid lines are theoretical predictions of Eq. (3) obtained without pump depletion. Let us first look at the data from the  $-2.4$ -psec/nm-km and 1-km fiber. The observed period is  $2.28$  psec for  $5.5$  W power [see Fig. 1(b) also]. This corresponds to the theoretical value for a choice of an effective area of  $97\text{ }\mu\text{m}^2$ , which is about 60% larger than the geometric core size.<sup>12</sup> The deviation of the data from the theoretical curve at higher powers is due to the pump depletion, as is illustrated in Fig. 1(c) and

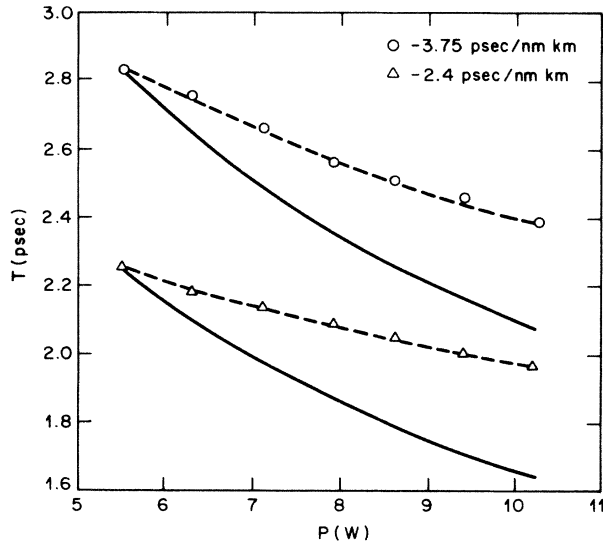


FIG. 3. The modulation period vs the input fiber power. The triangles and circles are the experimental data from the  $-2.4$ - and  $-3.75$ -psec/nm-km dispersion fibers, respectively. The solid lines show the theoretical predictions without the pump depletion.

1(d). Let us now look at the data from the  $-3.7$ -psec/nm-km and 1-km fiber. Notice that the period is 2.83 psec for 5.5 W, which is 1.24 times longer than 2.28 psec. The period ratio is exactly the square root of the dispersion ratio.

A threshold behavior, which is a signature of the exponential growth, is evident in the experiments. At low powers, no oscillation in the autocorrelation trace is found; at a certain higher power, large fluctuations in the autocorrelation trace are seen, which is due to the fluctuation in the laser power; at still higher powers, the autocorrelation trace becomes stable and exhibits oscillations with a power-dependent period. We make a rough check of the threshold-power dependence on fiber length. [Note that the loss in the longest fiber (2 km) is less than 25%.] Here, the threshold power is defined as the power for observing a power spectrum shown in Fig. 1(b) [i.e., about a gain of  $\exp(16)$ ]. The values are 10, 5.5, and 3 W for 0.5-, 1-, and 2-km lengths, respectively. The product of threshold power and length is approximately constant.

At power levels above 10 W for 1-km fibers, sidebands start to become asymmetric. This asymmetry is introduced by the Raman scattering, i.e., gain for the Stokes component (red-shifted) and absorption for the anti-Stokes component (blue-shifted).<sup>13</sup> Figure 4 shows the spectra when the Raman scattering becomes important [4(a)] and dominant [4(b)]. The threshold power for seeing the Raman effect is roughly inversely proportional to fiber length, as it should be.

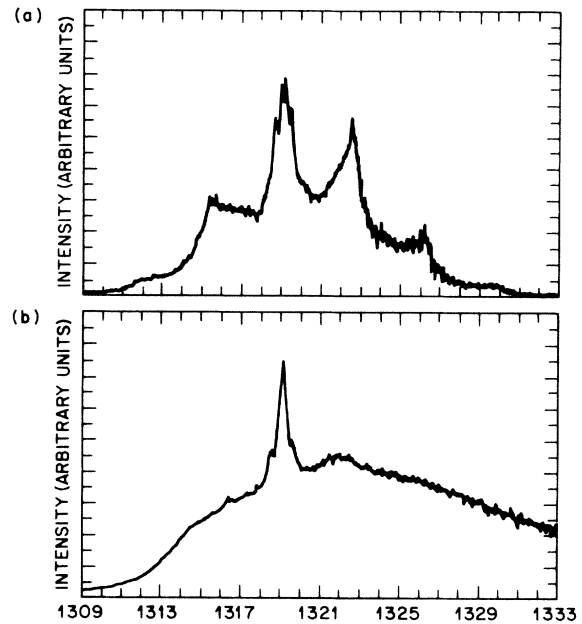


FIG. 4. The power spectra when the Raman gain (a) is important at 15 W and (b) becomes dominant at 25 W of the fiber power.

To prove that the modulational instability exists in a cw or a longer-pulse light wave, we perform the experiment using light from a  $Q$ -switched Nd-doped yttrium aluminum garnet laser, which puts out 1-kHz, 750-nsec (FWHM) pulses. The pulse duration is about 6 orders of magnitude longer than the modulation period. We observe similar spectrum shown in Fig. 1(b) at the same peak power. At slightly higher powers, the Brillouin scattering becomes dominant. The threshold power for the Brillouin scattering in this case is much larger than the reported value for a narrow-linewidth light source,<sup>14</sup> and is believed due to the multilongitudinal modes in the  $Q$ -switched pulse.

We note that the modulational instability is physically analogous to stimulated parametric four-wave mixing.<sup>15</sup> In the four-wave mixing usually a multimode fiber is required to satisfy the phase-matching condition, while in the modulational instability, the phase-matching condition is self-generated by the nonlinear change of index ( $\Delta n = \frac{1}{2}n_2|E|^2$ ) and the anomalous dispersion, and hence is susceptible of occurrence in single-mode fibers.

In conclusion, we have seen the modulational instability in the anomalous dispersion region of single-mode fibers. The absolute value and the dependence of the modulation frequency on the fiber parameters and power agree with the theory. Because of its high gain, the modulation instability may present a problem for the coherent fiber communication using wavelength division multiplexing. On the other hand, the

modulational instability may be used to generate a soliton train at high repetition rates.<sup>8</sup>

We would like to thank K. T. Nelson, W. R. Northover, and K. L. Walker for providing the fibers, and L. G. Cohen, S. R. Nagel, and R. H. Stolen for stimulating discussions and supports.

---

<sup>1</sup>G. B. Whitham, *J. Fluid Mech.* **22**, 273 (1965).

<sup>2</sup>A. Hasegawa, *Phys. Fluids* **15**, 870 (1972).

<sup>3</sup>L. A. Ostrovskiy, *Zh. Eksp. Teor. Fiz.* **51**, 1189 (1966) [*Sov. Phys. JETP* **24**, 797 (1967)].

<sup>4</sup>A. Hasegawa and W. F. Brinkman, *IEEE J. Quantum Electron.* **16**, 694 (1980).

<sup>5</sup>A. Hasegawa and F. D. Tappert, *Appl. Phys. Lett.* **23**, 142 (1973).

<sup>6</sup>R. H. Stolen and C. Lin, *Phys. Rev. A* **17**, 1448 (1978).

<sup>7</sup>The group velocity dispersion  $D$ , often measured in units of psec/nm-km, is given by  $D = (2\pi c/\lambda^2)\partial^2 k/\partial\omega^2$ , and includes both the material and the waveguide effects.

<sup>8</sup>Recently, A. Hasegawa [*Opt. Lett.* **9**, 288 (1984)] performed numerical studies of the induced modulational instability by injection of a periodic perturbation.

<sup>9</sup>K. C. Nelson, in *Technical Digest of the Topical Meeting on Optical Fiber Communication* (Optical Society of America, Washington, D.C., 1985), p. 98.

<sup>10</sup>To reduce further the zero-dispersion wavelength, a fiber with a  $W$ -type index profile is fabricated.

<sup>11</sup>The effective input modulation power (i.e., the product of the photon energy and the gain bandwidth) is 15 nW [see R. G. Smith, *Appl. Opt.* **11**, 2489 (1972)]. A gain of  $\exp(16)$  results in 0.13 W power, which agrees approximately with the observation.

<sup>12</sup>In a paper on an optical-fiber soliton experiment [L. F. Mollenauer, R. H. Stolen, and J. P. Gordon, *Phys. Rev. Lett.* **45**, 1095 (1980)], an effective area of 1.5 times the geometric area was used in analyzing the experimental results.

<sup>13</sup>R. H. Stolen, *Proc. IEEE* **68**, 1232 (1980).

<sup>14</sup>D. Cotter, *J. Opt. Commun.* **4**, 10 (1983).

<sup>15</sup>R. H. Stolen, J. E. Bjorkholm, and A. Ashkin, *Appl. Phys. Lett.* **24**, 308 (1974).

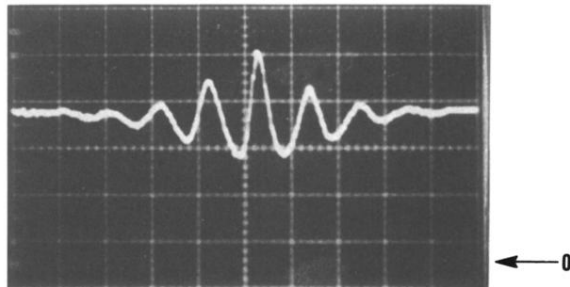


FIG. 2. A typical autocorrelation trace in the presence of the modulational instability. The zero delay occurs at the central maximum. The zero for the vertical axis is marked by an arrow. The interval between the oscillation peaks, which corresponds to the modulation period, is 2.2 psec in this case.